JOURNAL OF THEORETICAL AND APPLIED MECHANICS
49, 4, pp. 1151-1168, Warsaw 2011

CONTROL DESIGN OF SEMI-ACTIVE SEAT SUSPENSION SYSTEMS

Igor Maciejewski
Tomasz Krzyżyński

Koszalin University of Technology, Division of Mechatronics and Applied Mechanics, Koszalin, Poland; e-mail: igor.maciejewski@tu.koszalin.pl; tomasz.krzyzynski@tu.koszalin.pl

The paper deals with the control design of semi-active seat suspension systems. A semi-active vibration control strategy basing on the inverse dynamics of a spring or damper element and a primary controller is studied. The optimisation procedure proposed in the paper makes it possible to calculate controller settings and these, in turn, to define vibro-isolation properties of semi-active suspension systems.

Key words: vibration damping, semi-active suspension, control system

1. Introduction

Passive seat suspensions amplify vibration at frequencies close to their natural resonance frequencies. The first natural frequency of typical passive seats can be measured between 1 and 2 Hz. Active suspensions require large power supply and this is the main disadvantage of using such systems in practice extensively. Semi-active suspensions consume much less power than active suspensions, therefore they have received much attention in the literature (Ballo, 2007). A desirable performance of suspension systems can be archived using semi-active control, especially when some controllable dampers, like electro-rheological (ER) or magneto-rheological (MR) ones, are used (Du *et al.*, 2005; Maślanka *et al.*, 2007; Spencer *et al.*, 1997; Tsang *et al.*, 2006).

The design of vibro-isolating systems, constructed and manufactured at present, is a big challenge for engineers. This is due to opposite criteria that are involved in the design process (Alkhatiba *et al.*, 2004). For example, in the automotive industry, it is desired to reduce vibration of the cabin floor transmitted to the operator's seat. On one hand, dynamic forces transmitted

from the cabin floor to the seat should approach zero to protect machine operator's health. The Seat Effective Amplitude Transmissibility factor ($SEAT$) provides a simple numerical assessment of the seat isolation efficiency (Griffin, 1996)

$$SEAT = \frac{(\ddot{x}_w)_{RMS}}{(\ddot{x}_{sw})_{RMS}} \tag{1.1}$$

where $(\ddot{x}_{sw})_{RMS}$ is the frequency weighted root mean square value of the simulated input acceleration, $(\ddot{x}_w)_{RMS}$ is the frequency weighted root mean square value of the measured seat acceleration. On the other hand, the suspension deflection should approach zero in order to ensure the controllability of working machines. The suspension travel can be a simple numerical assessment of the seat performance as well. In this paper, the suspension travel is defined by the maximum relative displacement of the suspension system. Its value is calculated on the basis of the displacement signal in the time domain t as follows

$$(x - x_s)_{max} = \max_t(x - x_s) - \min_t(x - x_s) \tag{1.2}$$

where x is the seat displacement and x_s is the displacement caused by input vibration. Comfort criteria standardized for a selection of a trade-off between the $SEAT$ factor and the suspension travel $(x - x_s)_{max}$ cannot be found in the literature. However, the trade-off between conflicted requirements can be selected with the help of a multi-criteria optimisation.

2. Control system design

An evaluation of the control algorithms and strategies is required for the control of feedback loops in the semi-active suspensions. In order to control loops to work properly, the feedback loop must be properly tuned. Methods for tuning feedback loops and criteria for judging the loop tuning should be defined and used in modern control systems. The loop tuning can be achieved by appropriate selection of the controller settings and those correspond to the vibro-isolation properties of semi-active suspension systems.

2.1. Evaluation of primary controller

The simplified seat suspension model, that is composed of a single degree of freedom body mass, a linear spring and damper is used (Fig. 1). Such a

model has been extensively discussed in the literature and captures many essential characteristics of a real seat suspension system. The passive subsystem is applied to describe visco-elastic characteristics of the seat suspension system (for example with an air-spring and shock-absorber). The active subsystem is used to determine the desired force F_a that should be introduced into the visco-elastic suspension system in an active way.

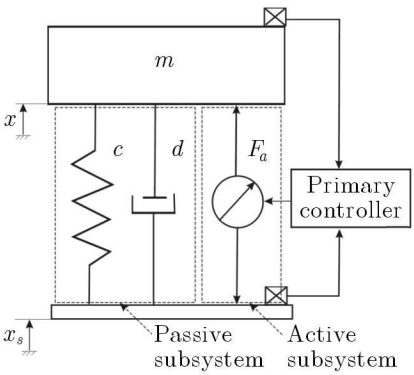

Fig. 1. Simplified model of the hybrid seat suspension system

The state space model of the hybrid seat suspension system (Fig. 1) can be obtained by using the LFT (Linear Fractional Transformation) technique (Gu *et al.*, 2005) and by grouping signals into sets of external inputs and outputs as well as into sets of controller inputs and outputs. Choosing the state variables as: $x_1 \coloneqq x - x_s$; $x_2 \coloneqq \dot{x}$, the disturbance caused by road roughness: $w_1 \coloneqq x_s$; $w_2 \coloneqq \dot{x}_s$ and the external input force of the suspension system $\boldsymbol{F}_a$, the state space equation of the hybrid seat suspension can be written in the following form

$$\dot{\boldsymbol{x}}(t) = \mathbf{A}\boldsymbol{x}(t) + \mathbf{B}_1\boldsymbol{w}(t) + \mathbf{B}_2\boldsymbol{F}_a(t) \tag{2.1}$$

where

$$\mathbf{A} = \begin{bmatrix} 0 & 1 \\ -\frac{c}{m} & -\frac{d}{m} \end{bmatrix} \qquad \mathbf{B}_1 = \begin{bmatrix} 0 & -1 \\ 0 & \frac{d}{m} \end{bmatrix} \qquad \mathbf{B}_2 = \begin{bmatrix} 0 \\ \frac{1}{m} \end{bmatrix} \tag{2.2}$$

In order to satisfy the performance requirement, the acceleration of the suspended mass $z_1 \coloneqq \ddot{x}$ and the suspension deflection $z_2 \coloneqq x - x_s$ are defined as controlled outputs. The output equation reads

$$\boldsymbol{z}(t) = \mathbf{C}_1\boldsymbol{x}(t) + \mathbf{D}_{11}\boldsymbol{w}(t) + \mathbf{D}_{12}\boldsymbol{F}_a(t) \tag{2.3}$$

where

$$\mathbf{C}_1 = \begin{bmatrix} -\frac{c}{m} & -\frac{d}{m} \\ 1 & 0 \end{bmatrix} \qquad \mathbf{D}_{11} = \begin{bmatrix} 0 & \frac{d}{m} \\ 0 & 0 \end{bmatrix} \qquad \mathbf{D}_{12} = \begin{bmatrix} \frac{1}{m} \\ 0 \end{bmatrix} \tag{2.4}$$

If the suspension deflection $y_1 \coloneqq x - x_s$ and the velocity of the suspended mass $y_2 \coloneqq \dot{x}$ are measurable, then the measurement equation can be written as follows

$$\boldsymbol{y}(t) = \mathbf{C}_2 \boldsymbol{x}(t) + \mathbf{D}_{21} \boldsymbol{w}(t) + \mathbf{D}_{22} \boldsymbol{F}_a(t) \tag{2.5}$$

where

$$\mathbf{C}_2 = \begin{bmatrix} 1 & 0 \\ 0 & 1 \end{bmatrix} \qquad \mathbf{D}_{21} = \begin{bmatrix} 0 & 0 \\ 0 & 0 \end{bmatrix} \qquad \mathbf{D}_{22} = \begin{bmatrix} 0 \\ 0 \end{bmatrix} \tag{2.6}$$

The controller is determined by formulating the state feedback control problem in the following form:

$$\boldsymbol{F}_a(t) = \mathbf{K} \boldsymbol{y}(t) = \mathbf{K} \mathbf{C}_2 \boldsymbol{x}(t) \tag{2.7}$$

where

$$\mathbf{K} = \begin{bmatrix} \boldsymbol{K}_1 & \boldsymbol{K}_2 \end{bmatrix} \tag{2.8}$$

is the output feedback gain vector to be designed.

However, the desired active force (Eq. (2.7)) has to be reproduced using controlled elements, i.e. by the spring with variable stiffness or by the damper with variable damping. In the semi-active suspension systems, it is well known that the spring and damper forces depend not only on their control signals but also on their actual working conditions, i.e. the actual deflection of the spring $x - x_s$ or the actual velocity of the damper $\dot{x} - \dot{x}_s$. If the actual spring deflection or the actual damper velocity are equal to nearly zero, then their forces reach zero and any control signal can produce the desired force. Therefore, the desired active force $\boldsymbol{F}_a$, that can be reproduced in the semi-active system in a better way, is calculated as follows

$$\boldsymbol{F}_a(t) = g_s \mathbf{K} \mathbf{C}_2 \boldsymbol{x}(t) \tag{2.9}$$

where g_s is the gain-scheduling function that shapes the desired active force to the actual working conditions of the spring or damper. This function is defined as follows

$$g_s = \begin{cases} \left| \dfrac{x - x_s}{(x - x_s)_n} \right| & \leftarrow \quad \text{controllable spring} \\ \left| \dfrac{\dot{x} - \dot{x}_s}{(\dot{x} - \dot{x}_s)_n} \right| & \leftarrow \quad \text{controllable damper} \end{cases} \tag{2.10}$$

where $(x-x_s)_n$ and $(\dot{x}-\dot{x}_s)_n$ are the nominal displacement and velocity of the controlled spring and damper, respectively. In Fig. 2, graphical representations of the functions described by Eqs. (2.10) are shown.

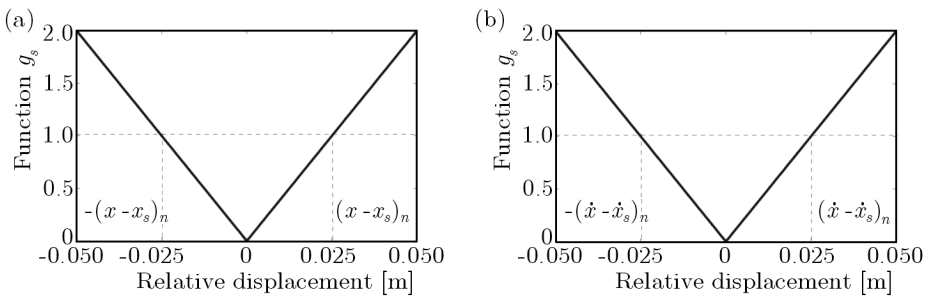

Fig. 2. Functions g_s for the spring control (a) and the damper control (b)

As follows from Fig. 2, the gain-scheduling function value equal to 1 is achieved for the actual displacement/velocity of controlled spring/damper element equal to the nominal value. In this case, the desired active force is not modified by the gain-scheduling function and such the force is reproduced in the semi-active system. If the actual displacement/velocity is greater two times than the nominal value, the desired active force is increased also 2 times by the gain-scheduling function (assuming a linear dependence). In this instance, the higher force is reproduced in the semi-active system. If the actual displacement/velocity is less than the nominal value, the lower force is reproduced in the semi-active system similarly.

2.2. Evaluation of secondary controller

If the desired active force F_a is determined then it has to be partly reproduced by the passive spring or damper element. This can be achieved using the force tracking control system that adjusts the controllable spring or damper. The force tracking control system can be handled by applying an internal force feedback or else by applying a reverse model of the spring or damper element (Maślanka *et al.*, 2007). The second approach is employed in this study, and in Fig. 3 the graphical illustration of such principle is presented.

The actual control signal u is calculated using a reverse model of the spring or damper element in the following form

$$u = \begin{cases} f(x - x_s, F_a) & \leftarrow \text{ spring force control} \\ f(\dot{x} - \dot{x}_s, F_a) & \leftarrow \text{ damper force control} \end{cases} \tag{2.11}$$

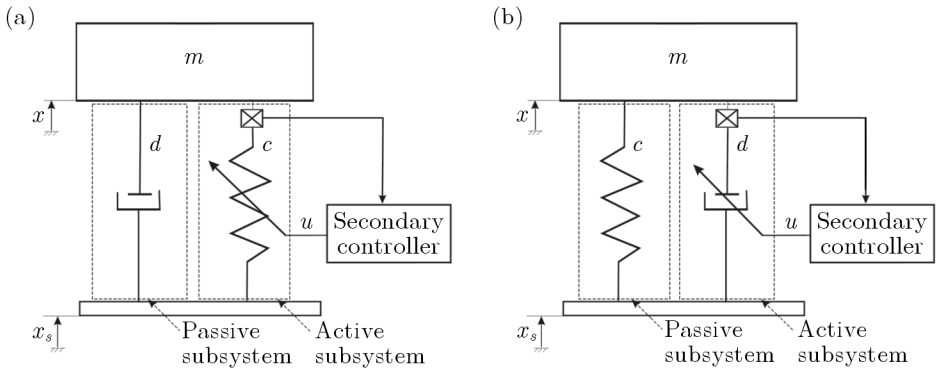

Fig. 3. Simplified models of the semi-active suspension system: with the controlled spring force (a) and with controlled damper force (b)

where $x - x_s$ and $\dot{x} - \dot{x}_s$ are the actual displacement and velocity of the controlled spring and damper, respectively.

The spring displacement, the damper velocity and the desired active force are the reverse model inputs. The model outputs are control signals to the spring and damper which should reproduce the desired active force in the semi-active system. Unfortunately, very often the force tracking control system efficiency is lowered by a phase shift in the feedback loop (Maślanka *et al.*, 2007). This effect might be caused by actuating time t_c of the spring or damper element. Therefore, the proportional-derivative (PD) controller is applied in order to speed up the overall control system. Finally, the output signal u_c of the PD controller, that controls the spring or damper element, is described as follows

$$u_c = t_c \dot{u} + u \tag{2.12}$$

where u is the control signal calculated on the basis of the reverse model (input to the PD controller).

The control signal u_c sent to the spring or damper should be restricted in the range of the minimum u_{min} and maximum u_{max} values. Therefore, although the desired force F_a can be of any value, the calculated input signal is constrained within the operating range

$$u_c = \begin{cases} u_{min} & \text{for} \quad u_c < u_{min} \\ u_c & \text{for} \quad u_{min} \leqslant u_c < u_{max} \\ u_{max} & \text{for} \quad u_c \geqslant u_{max} \end{cases} \tag{2.13}$$

2.3. Formulation of overall control system

In Fig. 4, the block diagram of the overall control system is presented. If the desirable active force is obtained according to the primary controller (Eq. (2.9)), then the desired force has to be approximately achieved by the spring or damper element with the calculated input signal using the reverse models (Eqs. (2.11)). In the control system proposed, any additional feedback loop from the actual spring/damper force is not required, because the force tracking is handled by applying the reverse model of the spring or damper element. The actuating time of the spring or damper element is eliminated by speeding up the control signal introduced to the the spring or damper (Eq. (2.12)). Due to the actual constraint of the input signal to the spring or damper element, the control signal is restricted within the range u_{min} and u_{max} (Eq. (2.13)).

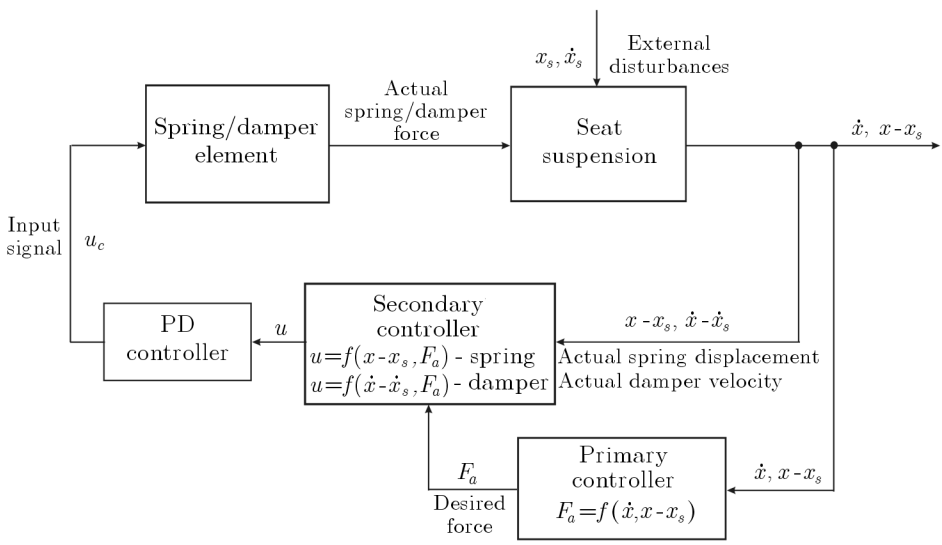

Fig. 4. Block diagram of the semi-active control for a seat suspension system

2.4. Multi-criteria optimisation of controller settings

1st step *Suspended mass range*

The vector of the suspended mass is defined as follows

$$\boldsymbol{m} = [m_1, \ldots, m_{n-1}, m_n] \qquad m_n - m_{n-1} = \text{const} \qquad n = 1, \ldots, i \tag{2.14}$$

Such a vector (in some software packages called the linearly spaced vector, e.g. MATLAB®) consists of equidistantly spaced elements whose the first value is m_1 and the last value is m_n, with the total number of n. The vector elements are defined as follows

$$\begin{aligned} m_1 &= m_{min} \\ &\dots \\ m_{n-1} &= m_{min} + \frac{n-1}{i-1}(m_{max} - m_{min}) \\ m_n &= m_{max} \end{aligned} \tag{2.15}$$

2nd step *Random starting points*

The vector of controller settings is given as

$$\mathbf{K} = [\boldsymbol{K}_1, \boldsymbol{K}_2, \dots, \boldsymbol{K}_p] \qquad p = 1, \dots, j \tag{2.16}$$

where p is the number of chosen controller settings. The ranges of controller settings have to be defined by the following vectors

$$\begin{aligned} \boldsymbol{K}_l &= [K_{l1}, K_{l2}, \dots, K_{lp}] \quad \leftarrow \quad \text{lower bounds} \\ \boldsymbol{K}_u &= [K_{u1}, K_{u2}, \dots, K_{up}] \quad \leftarrow \quad \text{upper bounds} \end{aligned} \tag{2.17}$$

where $\boldsymbol{K}_l$ and $\boldsymbol{K}_u$ are the vectors that contain the lowest and highest values of chosen controller settings, respectively. Using an uniform random number generator, the initial starting points may be expressed by

$$\begin{aligned} K_{s1} &= K_{l1} + (K_{u1} - K_{l1})\text{rand}(k) \\ K_{s2} &= K_{l2} + (K_{u2} - K_{l2})\text{rand}(k) \\ &\dots \\ K_{sp} &= K_{lp} + (K_{up} - K_{lp})\text{rand}(k) \end{aligned} \tag{2.18}$$

where k is the number of pseudo-random values (rand) drawn from the standard uniform distribution on the open interval $(0, \dots, 1)$.

3rd step *Minimization of particular optimisation criteria*

The separate minimizing processes of the $SEAT$ factor and the suspension travel $(x - x_s)_{max}$ are defined as follows

$$\begin{aligned} &\min_K SEAT(K) && \forall\, m_n \in \langle m_{min}; m_{max} \rangle, && n = 1, \dots, i \\ &\min_K (x - x_s)_{max}(K) && \forall\, m_n \in \langle m_{min}; m_{max} \rangle && n = 1, \dots, i \end{aligned} \tag{2.19}$$

with the bounds of controller settings

$$K_l \leqslant K \leqslant K_u \tag{2.20}$$

Such the optimisation procedure allows one to find extreme solutions which minimize the particular optimisation criteria separately:

- criterion coordinates $((x - x_s)_{max})_{max}$, $(SEAT)_{min}$ – minimum of the $SEAT$ factor,
- criterion coordinates $((x - x_s)_{max})_{min}$, $(SEAT)_{max}$ – minimum of the suspension travel.

The optimized systems are characterized by the best reduction of forces transmitted to the isolated body (minimum $SEAT$) or by the best limitation of the suspension travel (minimum $(x-x_s)_{max}$). In Fig. 5, a graphical representation of minimizing particular optimisation criteria is shown.

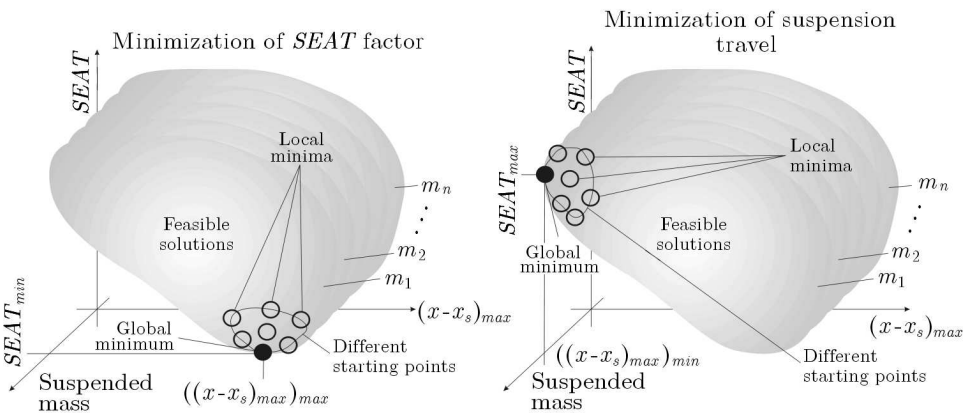

Fig. 5. Minimization of the particular optimisation criteria at different values of suspended masses

4th step *Minimization of conflicted vibro-isolation criteria*

In order to optimise both of the conflicted vibro-isolation criteria, minimization of the $SEAT$ factor (primary criterion) is defined as follows

$$\min_K SEAT(K) \qquad \forall\, m_n \in \langle m_{min}; m_{max} \rangle \qquad n = 1, \ldots, i \tag{2.21}$$

subject to the suspension travel $(x-x_s)_{max}$ that is transferred into a nonlinear inequality constraint

$$(x - x_s)_{max}(K) \leqslant ((x - x_s)_{max})_c \tag{2.22}$$

with the bounds of controller settings

$$K_l \leqslant K \leqslant K_u \tag{2.23}$$

The value $((x - x_s)_{max})_c$ determines a constraint of the maximum relative displacement of the suspension system. This value has to be included in the range of the suspension travel defined by the extreme solutions

$$((x - x_s)_{max})_{min} \leqslant ((x - x_s)_{max})_c \leqslant ((x - x_s)_{max})_{max} \tag{2.24}$$

where $((x-x_s)_{max})_{min}$ and $((x-x_s)_{max})_{max}$ are the minimum and maximum values of the suspension travel, respectively. An appropriate selection of the constraint value $((x - x_s)_{max})_c$ allows one to choose the vibro-isolation properties of the seat suspension system. In Fig. 6, a graphical representation of minimizatioi of the conflicted vibro-isolation criteria is shown. Each optimisation procedure should be repeated for the randomly generated starting points in order to find the global optimum of the seat suspension vibro-isolating properties.

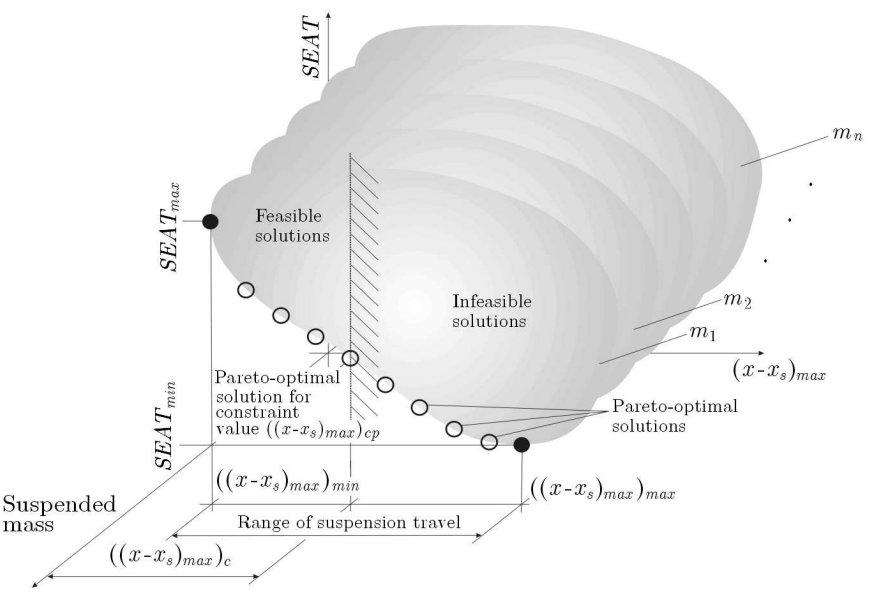

Fig. 6. Minimization of the conflicted vibro-isolation criteria at different values of suspended masses

3. Example: Multi-criteria optimisation of the seat suspension in semi-active vibration control

3.1. Optimisation object

In Fig. 7, a physical model of the semi-active seat suspension system containing a passive air-spring and a controllable magneto-rheological damper is shown. The equation of motion of the semi-active seat suspension takes a form similar as in the case of the passive seat suspension model (Maciejewski, 2009a). In that system, the pneumatic spring is connected to the additional air reservoir, therefore stiffness of the suspension system is rather low. However, damping of the suspension system is controlled using the MR damper.

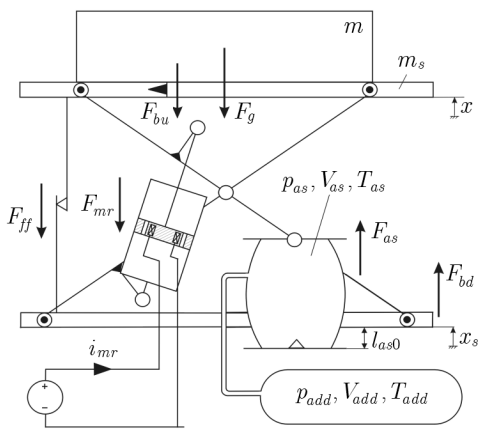

Fig. 7. Physical model of the semi-active seat suspension

The Bingham model presented by Spencer *et al.* (1997) is adopted in this study for the magneto-rheological damper using data obtained experimentally. In such a simplified model, the hysteresis loop of the MR damper is neglected and the description of the MR damper force contains components from a viscous damper and system friction only (cf. Fig. 8). The force is given by the following equation

$$F_{mr} = d_{mr}\Big(\frac{\dot{x} - \dot{x}_s}{\delta_d}\Big) + \alpha_{mr}\,\mathrm{sgn}\Big(\frac{\dot{x} - \dot{x}_s}{\delta_d}\Big) \tag{3.1}$$

where d_{mr} is the viscous damping coefficient, α_{mr} is the scale factor of the friction force, δ_d is the reduction ratio of the damper force. Basing on the experimental data, the least-square approximation method is employed to de-

termine the appropriate parameters d_{mr} and α_{mr} for the analytical model

$$d_{mr} = a_{mr}u + b_{mr} \qquad \alpha_{mr} = e_{mr}u^2 + f_{mr}u + g_{mr} \tag{3.2}$$

where a_{mr}, b_{mr}, e_{mr}, f_{mr} and g_{mr} are the polynominal coefficients expressed in respect to the input signal u. These coefficients are evaluated by means of additional MR damper measurements that were presented by Maciejewski (2009b).

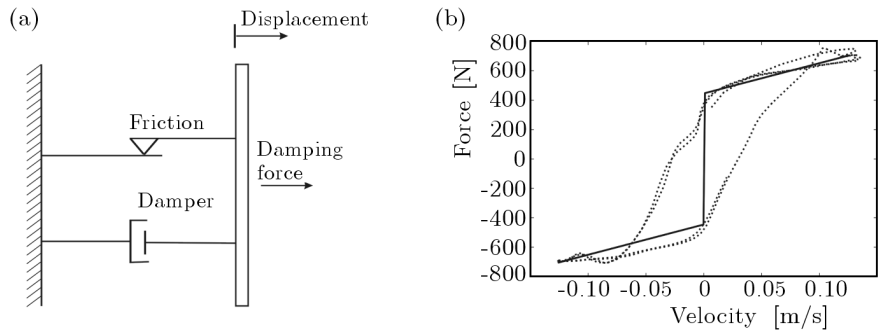

Fig. 8. (a) Bingham model of the magneto-rheological damper, (b) force of the magneto-rheological damper for control current 0.3 A: simulation (—), measurement (·····)

If the Bingham model is determined then the desirable force F_a can be realized by injecting an appropriate control signal into the MR damper in accordance with the actual piston velocity of the damper $u = f(F_a, \dot{x} - \dot{x}_s)$. The control signal u is calculated from Eqs. (3.1) and (3.2) with the measurable velocity $\dot{x} - \dot{x}_s$, and is given by

$$u = \frac{-f_{mr}\operatorname{sgn}\left(\frac{\dot{x}-\dot{x}_s}{\delta_d}\right) - a_{mr}\left(\frac{\dot{x}-\dot{x}_s}{\delta_d}\right) + \operatorname{sgn}\left(\frac{\dot{x}-\dot{x}_s}{\delta_d}\right)\sqrt{\Delta}}{2e_{mr}\operatorname{sgn}\left(\frac{\dot{x}-\dot{x}_s}{\delta_d}\right)} \tag{3.3}$$

with the function Δ that is calculated as

$$\begin{aligned}\Delta = &\left(f_{mr}\operatorname{sgn}\left(\frac{\dot{x}-\dot{x}_s}{\delta_d}\right) + a_{mr}\left(\frac{\dot{x}-\dot{x}_s}{\delta_d}\right)\right)^2 - \ldots \\ &+ 4e_{mr}\operatorname{sgn}\left(\frac{\dot{x}-\dot{x}_s}{\delta_d}\right)\left(g_{mr}\operatorname{sgn}\left(\frac{\dot{x}-\dot{x}_s}{\delta_d}\right) + b_{mr}\left(\frac{\dot{x}-\dot{x}_s}{\delta_d}\right) - \delta_d F_a\right)\end{aligned} \tag{3.4}$$

In Fig. 9, the graphical representation of the MR damper reverse model is shown. It should be noted that the MR damper is a semi-active device and the desired force F_a can be realized only if this force and the damper velocity

have the same sign. Then the calculated input signal of the MR damper varies in the range of 0 A (minimum value) and 1 A (maximum value) and depends on the actual value of the desired MR damper force and its actual velocity. If the desired force and damper velocity have sign opposite to each other then the input signal is settled to zero.

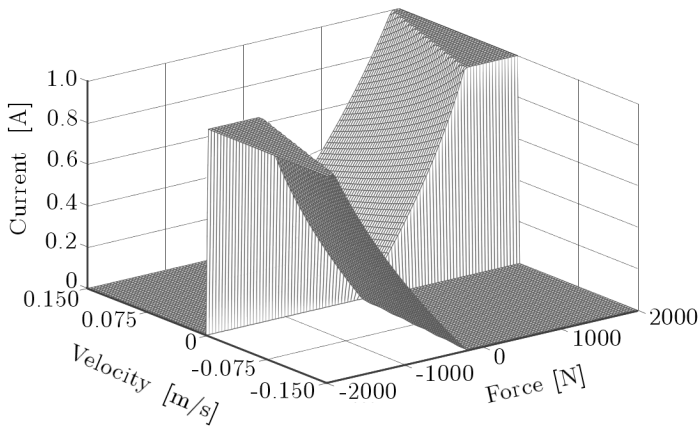

Fig. 9. Reverse model of the magneto-rheological damper $u = f(F_a, \dot{x} - \dot{x}_s)$

3.2. Decision variables and optimisation criteria

In order to enable controlling the vibro-isolation properties of a semi-active suspension, the controller settings and their ranges are taken as:

- the proportionality factor of the relative displacement feedback loop $K_{a1} = 5\text{-}50 \cdot 10^3\,\mathrm{N/m}$
- the proportionality factor of the absolute velocity feedback loop $K_{a2} = 0.5\text{-}5 \cdot 10^3\,\mathrm{Ns/m}$

The optimisation of the controller settings is realized using a simulation model of the semi-active system. The dynamic behaviour of the semi-active seat suspension is modelled in the MATLAB-Simulink® software package. The nonlinear ordinary differential equations (ODE) in the model are solved numerically using the fixed-step (step time of 1 ms) Bogacki-Shampine solver (Bogacki and Shampine, 1989). The optimisation procedure is performed for selected input vibrations that are specified in the International Standard (ISO 7096, 2000) for earth-moving machinery in particular spectral classes. In order to find the constrained minimum of the *SEAT* factor, a gradient-based optimisation algorithm with the Sequential Quadratic Programming (SQP) method is used (Gill *et al.*, 2005).

3.3. Optimisation results

In Fig. 10, the Pareto-optimal point distribution in conflicted criterion domains are shown. These results are obtained for the selected spectral classes of the excitation signal:

- EM3 – a signal at low frequencies and high amplitudes of vibration, representative for wheel loaders,
- EM5 – a signal at middle frequencies and middle amplitudes of vibration, representative for wheel dozers, soil compactors on wheels, backhoe loaders,
- EM6 – a signal at high frequencies and low amplitudes of vibration, representative for crawler loaders, crawler dozers.

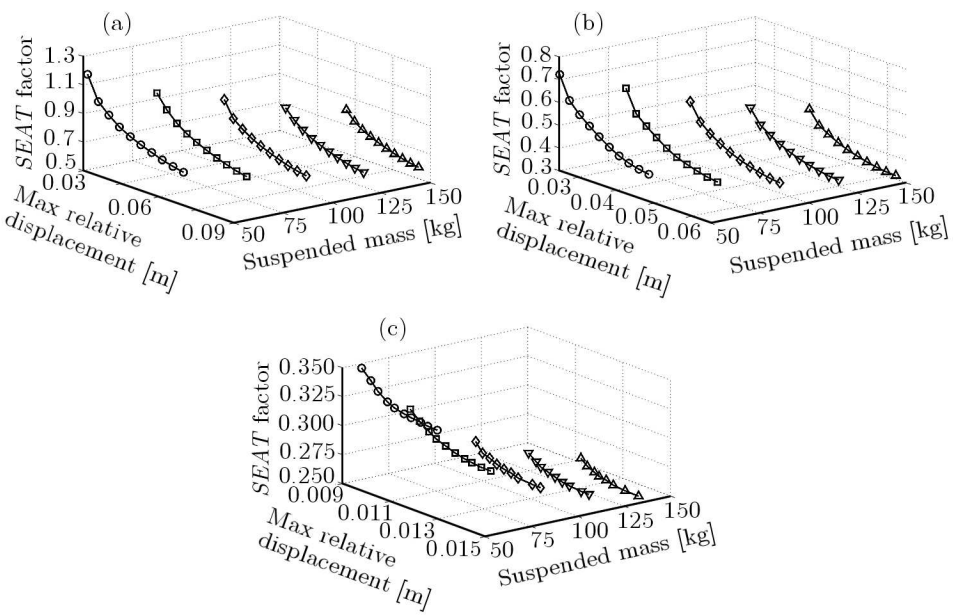

Fig. 10. Pareto-optimal point distribution for selected input vibrations: EM3 (a), EM5 (b), EM6 (c), mass load on the suspension system $m = 50\,\text{kg}$ ($\circ$), $m = 75\,\text{kg}$ ($\square$), $m = 100\,\text{kg}$ ($\diamond$), $m = 125\,\text{kg}$ (∇), $m = 150\,\text{kg}$ ($\triangle$)

In the example presented in this paper, ten Pareto-optimal solutions are found for the following values of the suspended mass: 50 kg, 75 kg, 100 kg, 125 kg and 150 kg. Each individual Pareto-optimal solution corresponds to a set of the decision variables which define different vibro-isolation characteristics of the semi-active suspension system.

3.4. Simulation and measurement results

In Fig. 11, point distributions (○) corresponding to the simulated Pareto-optimal solutions for the excitation signals: EM3, EM5 and EM6 are shown. The compromising solutions marked by the black circles (●), having a constraint imposed on the suspension travel, are experimentally investigated in this paper. The measurement results of the optimized semi-active suspension (▽) and of conventional passive suspension (△) are presented in the same figure. As follows from Fig. 11, the semi-active control significantly improves the seat suspension vibro-isolating properties for the excitation signals EM3 and EM5 (Fig. 11a,b) and only slightly for the excitation signal EM6 (Fig. 11c). The main improvement of the seat suspension dynamic behaviour is observed at the low frequency range. At higher frequencies, the friction force in the suspension system is dominating. In this frequency range both systems, the passive suspension and the semi-active suspension, yield almost the same response. In Fig. 12, the measured and simulated power spectral densities and transmissibility functions of the semi-active seat suspension for chosen excitation signals are presented.

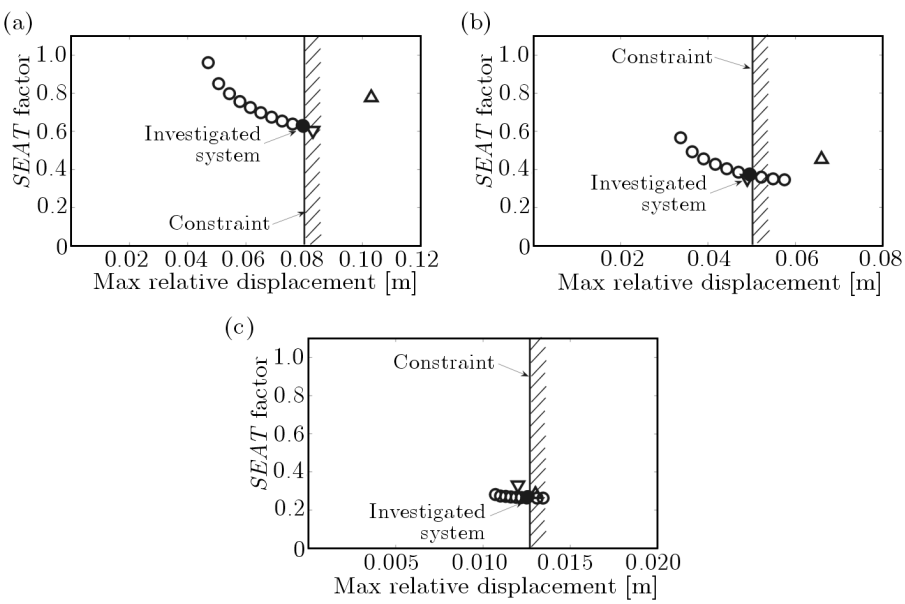

Fig. 11. Simulated Pareto-optimal point distribution (○) for selected input spectral classes: EM3 (a), EM5 (b), EM6 (c), measured conventional passive (△) and semi-active (▽) seat suspension systems, mass load on the suspension system $m = 100\,\mathrm{kg}$

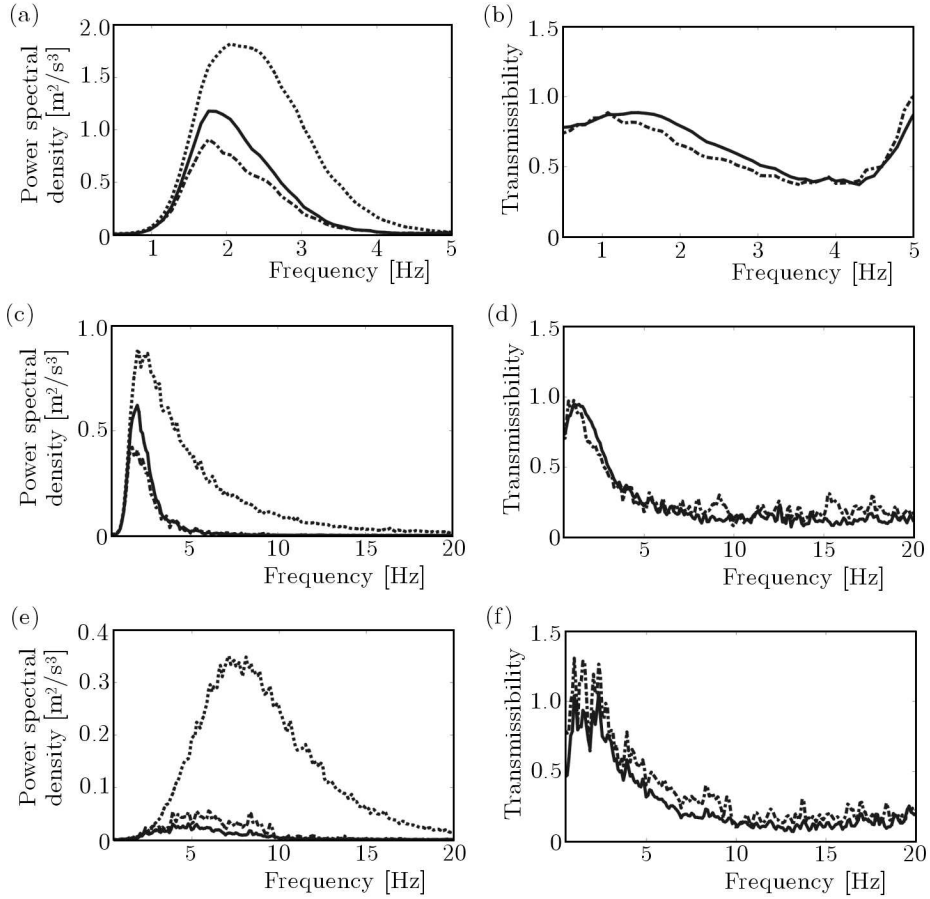

Fig. 12. Measured (- - -) and simulated (—) power spectral densities of the semi-active seat suspension for selected excitation signals (·····): EM3 (a), EM5 (c), EM6 (e), measured (-·-·-) and simulated (—) transmissibility functions of the semi-active seat suspension for selected excitation signals: EM3 (b), EM5 (d), EM6 (f), mass load on the suspension system $m = 100\,\mathrm{kg}$

However, the measurement results show that the dynamic behaviour of the semi-active seat suspension at optimized controller settings is close to the investigated Pareto-optimal system for each input spectral class (cf. Fig. 11). The conflicted optimisation criteria, i.e. the *SEAT* factor and the suspension travel $(x - x_s)_{max}$ are close to the calculated Pareto-optimal point distributions. It speaks well for the correctness of the proposed methodology for selecting the control system of the semi-active seat suspension.

4. Conclusions

The simulation and experimental results show that the presented methodology of the control system design allows one to define the overall structure of the semi-active seat suspension. Moreover, the proposed optimisation procedure assists to adjust the vibro-isolation properties of the semi-active suspension system. A stiff suspension system can be transformed to a soft suspension system by an appropriate selection of the controller settings. The proposed methodology for selecting the control system of semi-active suspension allows one to find desired dynamic behaviour of the seat for different requirements defined by machine operators. Each Pareto-optimal controller setting ensures the optimality of the control system for the conflicted vibro-isolation criteria.

References

1. Alkhatiba R., Nakhaie Jazarb G., Golnaraghi M.F., 2004, Optimal design of passive linear suspension using genetic algorithm, *Journal of Sound and Vibration*, **275**, 665-691
2. Ballo I., 2007, Comparison of the properties of active and semiactive suspension, *Vehicle System Dynamics*, **45**, 11, 1065-1073
3. Bogacki P., Shampine L.F., 1989, A 3(2) pair of RungeKutta formulas, *Applied Mathematics Letters*, **2**, 4, 321-325
4. Chen Y., 2009, Skyhook surface sliding mode control on semi-active vehicle suspension system for ride comfort enhancement, *Engineering*, **1**, 1-54
5. Dong X., Yu M., Liao Ch., Chen W., 2009, Comparative research on semi-active control strategies for magneto-rheological suspension, *Nonlinear Dynamincs*, DOI 10.1007/s11071-009-9550-8 (published online)
6. Du H., Sze K.Y., Lam J., 2005, Semi-active H-inf control of vehicle suspension with magneto-rheological dampers, *Journal of Sound and Vibration*, **283**, 981-996
7. Gill P.E., Murray W., Wright M.H., 1981, *Practical Optimization*, Academic Press, London
8. Griffin M.J., 1996, *Handbook of Human Vibration*, Elsevier Academic Press, London
9. Gu D., Petkov P., Konstantinov M., 2005, *Robust Control Design with MATLAB*, Springer, Berlin

10. ISO 7096, 2000, *Earth-moving machinery – Laboratory evaluation of operator seat vibration*

11. Maciejewski I., 2009a, On modelling of working machines seat suspension, *Logistyka*, **3** (CD publication) [in Polish]

12. Maciejewski I., 2009b, Vibro-isolation properties of semi-active seat suspension with the magneto-rheological damper, *Pomiary, Automatyka, Kontrola*, **9**, 727-730 [in Polish]

13. Maślanka M., Sapiński B., Snamina J., 2007, Experimental study of vibration control of a cable with an attached MR damper, *Journal of Theoretical and Applied Mechanics*, **45**, 4, 893-917

14. Preumont A., 2002, *Vibration Control of Active Structures An Introduction*, Kluwer Academic Publishers, London

15. Spencer Jr. B.F., Dyke S.J., Carlson J.D., 1997, Phenomenological model for magnetorheological dampers, *Journal of Engineering Mechanics* **123**, 3, 230-238

16. Tsang H., Su R., Chandler A., 2006, Simplified inverse dynamics models for MR fluid dampers, *Engineering Structures*, **28**, 327-341

Projekt systemu sterowania semi-aktywnym układem zawieszenia siedziska

Streszczenie

w pracy przedstawiono sposób projektowania systemu sterowania semi-aktywnym układem zawieszenia siedziska. Analizowano algorytm sterowania semi-aktywnego, który bazuje na modelu odwrotnym elementu sprężystego lub tłumiącego oraz na kontrolerze głównym. Procedura optymalizacji zaproponowana w pracy dodatkowo wspomaga dobór nastaw regulatora, ktore to nastawy definiują właściwości wibroizolacyjne semi-aktywnego układu zawieszenia.

Manuscript received November 8, 2010; accepted for print February 7, 2011